

Could Momordica Charantia Be Effective In The Treatment of COVID19?

Burak Tüzün^{1,a,*}, Koray Sayın^{2,b}, Hilmi Ataseven^{3,c}

¹ Plant and Animal Production Department, Technical Sciences Vocational School of Sivas, Sivas Cumhuriyet University, Sivas, Türkiye

² Department of Chemistry, Faculty of Science, Sivas Cumhuriyet University, Sivas, Türkiye

³ Department of Gastroenterology, Faculty of Medicine, Sivas Cumhuriyet University, Sivas, Türkiye

*Corresponding author

Research Article

History

Received: 19/10/2021

Accepted: 22/05/2022

Copyright



©2022 Faculty of Science,
Sivas Cumhuriyet University

btuzun@cumhuriyet.edu.tr
hilmiataseven@yahoo.com

ABSTRACT

One of the deadliest diseases is the SARS-CoV-2 virus, today. The rate of spread of this virus is very high. Momordica Charantia extracts studied for this virus. The inhibitory activities of 96 components in the extract of Momordica Charantia were compared against the SARS-CoV-2 virus. Molecular docking method was initially used for this comparison. ADME/T analysis of the inhibitors with the highest inhibitory activity was performed using the results obtained from these calculations. The molecular docking calculations of the molecule with the highest inhibitory activity were tried to be supported by MM-PBSA calculations. The molecular mechanics Poisson-Boltzmann surface binding free energy values of area (MM-PBSA) calculations study interactions between inhibitor molecules and SARS-CoV-2 virus proteins at 100 ps. Finally, the molecules with the highest inhibitory activity were compared with FDA approved drugs. As a result of the made molecular docking calculations, the docking score parameter is Karaviloside III with -9.36, among the extracts of momordica charantia, which has the most negative value. The Gibbs free energy value of the Karaviloside III against 6X6P protein with the best docking score value was calculated. This value is -477143.61±476.53. As a result of the comparison of inhibitory activities of extracts of Momordica charantia against SARS-CoV-2 virus, it has been observed that the Karaviloside III molecule has higher inhibitory activity than other melodies and FDA drugs.

Keywords: SARS-CoV-2, Molecular docking, COVID-19, Momordica charantia, ADME/T.

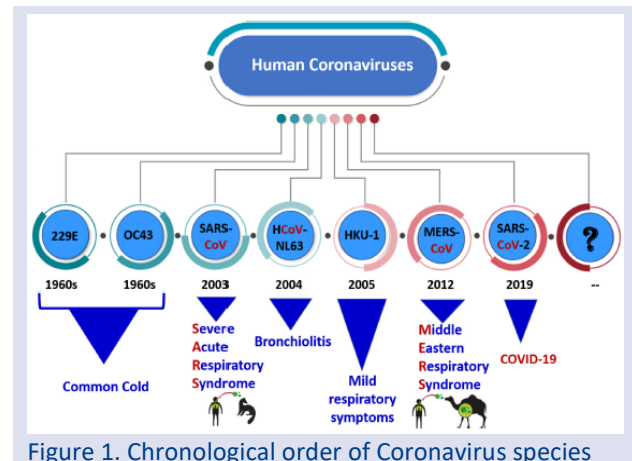
<https://orcid.org/0000-0002-0420-2043>
<https://orcid.org/0123-4578-9012-3457>

ksayin@cumhuriyet.edu.tr <https://orcid.org/0000-0001-6648-5010>

Introduction

Severe Acute Respiratory Syndrome Coronavirus 2 (SARS-CoV-2), which started in Wuhan city of China and affected the whole world, is currently the most contagious and effective virus [1]. This virus started in the last month of 2019, infected 23 million people in 7 months, and caused the death of 850 thousand people. This infection was declared a pandemic by the world health organization (WHO) in March 2020. SARS-CoV-2 is an enveloped positive-sense single-stranded ribonucleic acid (RNA) virus. It is a dangerous virus that can spread from person to person through droplet exchange while coughing, talking, and sneezing. The upper respiratory tract's symptoms such as fever, dry cough, nausea, head and throat pain, and runny nose are in the foreground for this virus [2]. In patients, all of these symptoms appear between 3 and 14 days. People with low immune systems such as diabetes, heart problems, cancer, asthma, and organ transplantation are reported to show acute symptoms [2]. When the virus's incubation period ends, these mild symptoms worsen and begin to accumulate water in the lungs. Subsequently, the virus leads to respiratory failure and finally causes the patient to become pneumonia. When the disease reaches this level, it is challenging for the patient to recover [3].

Another name for SARS-CoV-2 disease is COVID-19. This disease is the seventh coronavirus transmitted to humans.



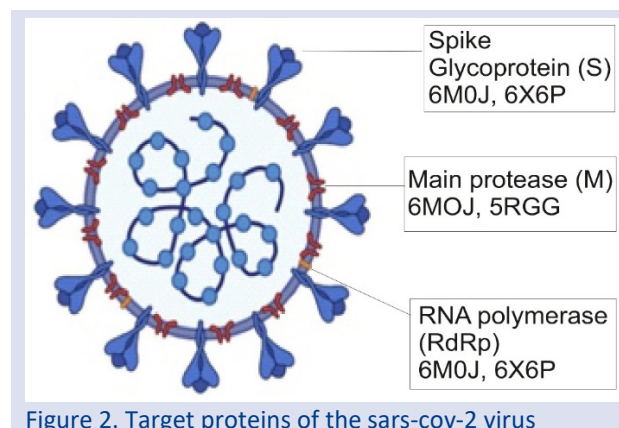
This virus is classified under four main headings: alfa, beta, gamma, and delta [4]. The order of the coronavirus types by years is shown in Figure 1. The six known before that are HCoV-229E (Human coronavirus 229E), HCoV-OC43 (Human coronavirus OC43), SARS-CoV (Severe acute respiratory syndrome- coronavirus), HCoV-NL63 (Human coronavirus NL63), HCoV-HKU-1 (Human coronavirus-HKU-1), MERS-CoV (Middle East respiratory syndrome coronavirus) [5]. Although SARS-CoV-2 triggers diseases in different and multiple organ systems in animals, it generally targets humans' respiratory systems. Although HCoV-229E, HCoV-OC43, SARS-CoV, HCoV-NL63, and

HCoV-HKU-1 cause upper respiratory tract discomfort with mild symptoms, SARS-CoV, MERS-CoV, and SARS-CoV-2 have serious and dangerous diseases. It is classified as the high pathogen that can cause [3,6]. The membrane receptor of host cells plays an essential role in the entry of coronaviruses into host cells and their pathogenesis. The coronavirus recognizes host receptors with its envelope-anchored spike (S) protein and binds with this protein's help. It then enters the cell by binding the host and viral membranes [7]. It was seen in many experimental and theoretical studies conducted before that, it was observed that the genome sequences of SARS-CoV-2 were 80% similar to other coronaviruses [8]. But SARS-CoV-2 infection rate is more than ten times higher [9]. The coronavirus genome consists of four main structural proteins. These are (1) the spike (S) protein, (2) nucleocapsid (N) protein, (3) membrane (M) protein, and (4) the envelope (E) protein [10].

Many theoretical studies have shown that it has been shown that four basic proteins within the SARS-CoV-2 virus are focused. The first is the main protease of the coronavirus 3CLpro and PLpro. The antiviral drug lopinavir [11,12] is used. The second is the RNA-dependent RNA polymerase [(RdRp), also called nsp12] protein of the coronavirus. Remdesivir [11], ribavirin [11,13], and favipiravir [14] are used as antiviral drugs. The third is the coronavirus s protein (viral spike glycoprotein). Arbidol [15] is used as an antiviral drug. The fourth and last is the ACE 2 protein of the coronavirus. Arbidol [15] is used as an antiviral drug.

Momordica charantia has many major components. The most important of these main components are cucurbitacins, sterols, triterpenoids, and vicine [16]. Momordica charantia has been used for centuries, particularly in the treatment of stomach diseases. The fruit of Momordica charantia is separated when ripe, giving orange-yellow fruits. In recent years, research has been carried out for cancer treatment with Momordica charantia, whose homeland is considered to be India. With Momordica charantia, natural support can be provided for digestive system diseases. The active ingredient called quarantine in Momordica charantia is effective in gastritis, stomach ulcer, reflux problems. Momordica charantia reduces the number of Helicobacter Pylori bacteria, suppressing their activity, and preventing their growth. It is effective against stomach and intestinal infections with its anti-inflammatory properties. An article published in "Current Molecular Medicine" in May 2011 wrote that Momordica charantia contains more than 20 bioactive compounds that increase its therapeutic value. Nearly 100 in vitro studies have proven the blood sugar lowering effect of Momordica charantia to date. In the June 2001 issue of the journal "Planta Medica" published a study demonstrating the capacity of Momordica charantia to inhibit HIV [17]. The June 2009 issue of the "Pharmaceutical Research" newsletter also reported that Momordica charantia inhibits cancer cells' growth and promotes cancer cell death without touching healthy cells [18]. The October 2010 issue of "Cancer Science" included

a study stating that Momordica charantia extract prevents carcinogenic cells from spreading from prostate tumors to the lung [19].



In the study of Ahamad et al., Momordica charantia found 96 components. These ninety-six molecules are given in supplementary data file. However, the inhibitory effects of 96 molecules of Momordica charantia against proteins of spike glycoprotein (PDB ID: 6M0J, 6X6P), main protease (PDB ID: 5RGG, 7BUY), and RNA dependent RNA polymerase (RdRp) (PDB ID: 7BV1, 7BV2) of the SARS-CoV-2 virus were compared by molecular docking calculations, are represented in Figure 2. The molecular mechanics Poisson-Boltzmann surface binding free energy values of area (MM-PBSA) calculations study interactions between inhibitor molecules and SARS-CoV-2 virus proteins at 100 ps. Afterward, ADME/T analysis of the molecules with the highest inhibitory activity among these 96 molecules was performed.

Material and Methods

Previous theoretical studies show that the inhibitory properties of the molecules formed by many components of the Momordica Charantia against SARS-CoV-2 proteins were compared using molecular docking, which is one of the most used methods. Inhibitory activities were compared using the numerical value obtained from the interactions between molecules and SARS-CoV-2 proteins by molecular docking method. Active regions of many SARS-CoV-2 proteins are determined by calculations. In this study, molecular docking calculations were made to compare the inhibitory activities with the molecules of the Momordica Charantia.

Molecular docking calculations to calculate the inhibitory activities of 96 molecules studied were performed using the Maestro Molecular modeling platform (version 12.2) by Schrödinger. For these calculations, proteins and 96 pieces of Momordica Charantia molecules studied must be prepared. In docking calculations, a different process is performed for molecules at each stage. First, it was used from the Gaussian software program [20] to obtain optimized structures of molecules with extension *.sdf were created using these structures.

All calculations were made with the Maestro Molecular modeling platform (version 12.2) by Schrödinger, LLC [21]. The Maestro Molecular modeling platform (version 12.2) by Schrödinger comes together from many modules. In the first module, the protein was prepared and the active site of the protein was found. The protein preparation module [22,23] is used. In the next module, the LigPrep module [24,25] was used to do the necessary operations for docking calculations of molecules.

For the next step, The Glide ligand docking module [26] was used to calculate interactions between the 96 therapeutic agents studied and the SARS-CoV-2 progeny. In this module, the OPLS3e method was used in all calculations for docking calculations of molecules and proteins. Numerical values of many parameters obtained as a result of molecular docking calculations using this module are used. After the docking calculations, studied 96 therapeutic agents were made ADME/T analysis (absorption, distribution, metabolism, excretion, and toxicity) so that they could become drugs in the future. The Qik-prop module [27] of the Schrödinger software was used for ADME/T analysis.

Molecular mechanics Poisson-Boltzmann surface area (MM-PBSA) calculations were performed for 6X6P protein and molecule 4a. For MM-PBSA calculations, Nanoscale Molecular Dynamics (NAMD) [28] and Visual Molecular Dynamics (VMD) [29] software programs were calculated all calculations. Binding free energy provides an overview of biomolecular interactions between protein and inhibitor. The binding energy of protein and inhibitor constitutes of potential energy, polar and non-polar solvation energies. In these calculations, the free binding energy and the total free energy of the protein, inhibitors, and inhibitor-protein complex were calculated respectively.

$$\Delta G_{\text{Binding}} = \Delta G_{\text{complex}} - (\Delta G_{\text{protein}} + \Delta G_{\text{inhibitor}})$$

where; $\Delta G_{\text{Binding}}$ is the binding free energy, $\Delta G_{\text{complex}}$, $\Delta G_{\text{protein}}$, and $\Delta G_{\text{inhibitor}}$ demonstrates the total free energy of the protein-ligand complex and total free energies of the isolated protein and ligand, respectively. Each term in the above equation consists of the combination of many energy components. These are composed of many components such as van der Waals energy, electrostatic energy, and polar contribution.

Results and Discussion

The ninety-three molecules of *Momordica charantia* will inhibit three different proteins of the SARS-CoV-2 virus. Three different SARS-CoV-2 virus proteins were taken into consideration, spike glycoprotein, main protease, and RNA dependent RNA polymerase proteins. It should be well known that the more that these 96 molecules interacts with the three different proteins of the SARS-CoV 2 virus, the most inhibition effect would be. The molecule with the most inhibition effect will stop the SARS-Cov-2 virus from entering the cell. Hence, replication of the SARS-Cov-2 virus in human metabolism would be inhibited.

Ninety-three molecules of the studied *Momordica charantia* were investigated by the molecular docking method against the SARS-CoV-2 virus's proteins. As a result of these calculations, many parameters about the inhibitors were calculated. These parameters provide much information about inhibitors' inhibitory properties against SARS-CoV-2 virus proteins [23]. As a result of molecular docking calculations, the most important parameter among the obtained parameters is the docking score parameter. This parameter is used to explain the interaction between inhibitors and proteins. It should be well known that if the interaction between the inhibitor and the proteins increases, the inhibitor's activity increases [25]. This increase in interaction causes the SARS-CoV-2 virus to inhibit the protein.

There are many more parameters obtained from docking calculations. These parameters are used to explain the interactions between the inhibitor and SARS-CoV-2 proteins. These parameters are Glide hbond, Glide evdw, and Glide ecoul. These parameters provide information about the number of chemical interactions that occur between the inhibitor and the proteins. These parameters give a numerical expression of hydrogen bonding, Van der Waals interactions, and Coulomb interactions occurring between inhibitors and proteins [30-32]. Apart from these parameters, there are Glide emodel, Glide energy, and Glide einternal parameters. All of these parameters explain the interaction of molecules with inhibitors. Table 1 shows the numerical values of the five inhibitors with the highest inhibitory activity among 96 inhibitors for all parameters [33].

As a result of molecular docking calculations, the best inhibitors for the three active protein regions of the SARS-CoV-2 virus are given in Table 1. These inhibitors are 4-Methoxybenzoic Acid (1a), Gypsogenin (2a), Momordicine I (3a), Karaviloside III (4a), and Charantoside II (5a). The interactions of the highest inhibitory activity molecules of 96 inhibitor molecules of *Momordica charantia* with the studied proteins are given in Figure 3-8.

Table 1. Numerical values of the docking parameters of molecule against enzymes

Protein	Parameters	1a	2a	3a	4a	5a
6MOJ	Docking score	-2.50	-3.34	-2.26	-	-
	Glide ligand efficiency	-0.23	-0.10	-0.07	-	-
	Glide evdw	-14.14	-18.81	-19.87	-	-
	Glide ecoul	-6.99	-7.75	-9.24	-	-
	Glide energy	-21.13	-26.55	-29.11	-	-
	Glide einternal	0.04	2.41	5.20	-	-
	Glide emodel	-24.41	-26.83	-36.67	-	-
	Glide hBond	-0.31	-2.09	-1.48	-	-
6X6P	Docking score	-3.63	-7.32	-7.17	-9.36	-8.57
	Glide ligand efficiency	-0.33	-0.22	-0.21	-0.21	-0.18
	Glide evdw	-11.83	-26.94	-32.43	-28.75	-22.25
	Glide ecoul	-5.27	-3.49	-1.61	-9.01	-11.31
	Glide energy	-17.10	-30.44	-34.04	-37.76	-33.55
	Glide einternal	3.35	7.70	0.00	15.62	0.00
	Glide emodel	-17.66	53.35	-46.09	10.46	26.41
	Glide hBond	-1.94	-1.95	-1.06	-2.96	-2.40
5RGG	Docking score	-2.65	-4.37	-6.44	-8.77	-7.09
	Glide ligand efficiency	-0.24	-0.13	-0.19	-0.19	-0.15
	Glide evdw	-15.39	-29.03	-32.83	-20.59	-31.84
	Glide ecoul	-2.62	-6.09	-7.87	-19.36	-11.57
	Glide energy	-18.01	-35.12	-40.70	-39.96	-43.41
	Glide einternal	0.83	2.27	5.20	13.26	11.53
	Glide emodel	-21.91	-44.43	-51.48	-58.62	-55.18
	Glide hBond	-0.60	-0.82	-1.33	-5.38	-3.05
7BUY	Docking score	-3.12	-4.71	-4.52	-7.35	-7.27
	Glide ligand efficiency	-0.28	-0.14	-0.13	-0.16	-0.15
	Glide evdw	-15.10	-21.68	-22.73	-31.55	-37.42
	Glide ecoul	-2.14	-8.80	-6.06	-12.79	-7.02
	Glide energy	-17.24	-30.48	-28.79	-44.33	-44.44
	Glide einternal	0.00	1.23	7.86	10.51	0.00
	Glide emodel	-21.91	-28.26	5.76	-32.36	-54.28
	Glide hBond	-0.35	-2.16	-1.32	-3.41	-3.03
7BV1	Docking score	-3.66	-4.64	-5.14	-8.42	-7.98
	Glide ligand efficiency	-0.33	-0.14	-0.15	-0.19	-0.17
	Glide evdw	-13.52	-33.47	-23.84	-26.83	-28.73
	Glide ecoul	-5.87	-0.58	-8.77	-18.24	-16.73
	Glide energy	-19.39	-34.05	-32.61	-45.07	-45.46
	Glide einternal	4.43	1.72	22.87	9.81	7.35
	Glide emodel	-21.47	-43.44	-18.74	-53.91	-55.02
	Glide hBond	-1.89	-1.41	-2.22	-3.55	-3.51
7BV2	Docking score	-1.70	-4.18	-4.68	-	-
	Glide ligand efficiency	-0.15	-0.12	-0.14	-	-
	Glide evdw	-14.92	-28.86	-18.62	-	-
	Glide ecoul	3.65	1.04	-5.51	-	-
	Glide energy	-11.28	-27.82	-24.13	-	-
	Glide einternal	0.43	0.49	5.70	-	-
	Glide emodel	-12.60	-32.52	-28.47	-	-
	Glide hBond	-0.30	-2.01	-1.92	-	-

After comparing the inhibitory activity of inhibitors against the protein, ADME/T analysis was performed to theoretically predict the five molecules' effects and responses with the highest inhibitory activity in human metabolism. To predict the effects and responses of inhibitors on organs and tissues in the human body from the numerical values obtained with this theoretical analysis. The numerical values of all the inhibitors' calculated parameters with this analysis are given in Table 2 in detail.

As a result of molecular docking calculations, there are two most essential parameters obtained due to ADME/T analysis for inhibitors, which are The RuleOfFive [34,35] and RuleOfThree [36] parameters. These two parameters constitute a combination of many parameters. Therefore, the numerical value of this parameter is required to be zero. Each other parameter gives the numerical value of the effects of inhibitor molecules on different organs and tissues.

Table 2. ADME properties of molecules

	1a	2a	3a	4a	5a	Reference Range
mol_MW	152	471	473	635	663	130-725
dipole (D)	3.9	4.7	4.0	7.1	6.4	1.0-12.5
SASA	347	703	779	979	986	300-1000
FOSA	93	534	613	789	797	0-750
FISA	107	151	148	178	146	7-330
PISA	147	17	17	11	43	0-450
WPSA	0	0	0	0	0	0-175
volume (A ³)	539	1420	1526	1966	2008	500-2000
donorHB	1	1	3	5	4	0-6
accptHB	2.8	4.7	7.1	12.7	14.4	2.0-20.0
glob (Sphere =1)	0.9	0.9	0.8	0.8	0.8	0.75-0.95
QPpolrz (A ³)	15.5	48.9	49.9	64.3	66.3	13.0-70.0
QPlogPC16	5.3	12.7	14.1	18.9	18.9	4.0-18.0
QPlogPoct	7.9	20.6	24.7	35.8	35.8	8.0-35.0
QPlogPw	6.0	8.0	12.3	20.3	20.5	4.0-45.0
QPlogPo/w	2.0	5.8	4.6	4.5	4.5	-2.0-6.5
QPlogS	-1.6	-6.8	-6.3	-6.9	-6.6	-6.5-0.5
CIQlogS	-1.6	-7.0	-5.9	-6.8	-6.9	-6.5-0.5
QPlogHERG	-1.7	-1.9	-4.5	-5.2	-5.3	*
QPPCaco (nm/sec)	243	92	387	202	410	**
QPlogBB	-0.4	-1.0	-1.4	-2.2	-1.8	-3.0-1.2
QPPMDCK (nm/sec)	136	48	177	88	189	**
QPlogKp	-2.8	-4.0	-3.4	-3.5	-2.8	Kp in cm/hr
IP (ev)	9.5	9.5	9.7	9.6	9.6	7.9-10.5
EA (eV)	0.4	-0.5	-0.6	-1.0	-0.9	-0.9-1.7
#metab	1	3	6	8	9	1-8
QPlogKhsa	-0.6	1.3	0.9	0.7	0.6	-1.5-1.5
Human Oral Absorption	3	1	1	1	1	-
Per. Human Oral Absorp.	81	83	100	82	87	***
PSA	59	94	84	125	116	7-200
RuleOfFive	0	1	0	1	1	Maximum is 4
RuleOfThree	0	1	1	2	2	Maximum is 3
Jm	9.6	0.0	0.0	0.0	0.0	-

Table 3. Representation of calculated parameters (kcal/mol) and standard deviation values of 6X6P protein and molecule 5a

Time (ps)	VDW		Kinetic		Potential		Gibbs binding free energy	
5000	37115.05	±6595.83	126302.61	±13544.26	-608437.17	±19585.05	-481644.11	±33037.00
10000	36094.54	±623.60	127085.12	±578.59	-603639.74	±998.39	-476081.47	±1441.35
15000	35723.95	±139.42	127073.28	±475.47	-603548.75	±488.83	-475969.93	±586.26
20000	36086.30	±620.05	127484.33	±347.71	-604501.37	±413.03	-476526.19	±462.71
25000	36155.52	±745.37	126908.49	±446.19	-604120.55	±421.86	-476727.22	±490.26
30000	34966.01	±571.37	127412.85	±383.23	-604979.05	±457.17	-477087.87	±515.18
35000	35187.36	±176.06	127982.60	±434.36	-603731.49	±595.22	-475245.12	±708.41
40000	34767.18	±42.96	127740.12	±366.03	-604973.83	±608.04	-476719.04	±657.72
45000	35430.36	±217.40	127164.10	±411.80	-604112.24	±547.16	-476449.45	±618.66
50000	35294.45	±647.40	126133.13	±473.90	-604967.54	±519.74	-478338.59	±583.24
55000	35355.61	±373.00	127982.63	±413.69	-604620.99	±626.82	-476140.86	±686.34
60000	35700.43	±356.67	127658.33	±417.18	-605190.27	±442.57	-477014.96	±392.80
65000	35845.87	±382.39	127679.02	±408.40	-605115.02	±415.79	-476944.97	±419.74
70000	35432.53	±381.52	127188.26	±345.76	-604172.07	±493.60	-476523.05	±469.70
75000	35632.89	±38.03	128005.92	±384.58	-605709.68	±474.10	-477214.31	±491.85
80000	35291.97	±217.59	127035.33	±389.65	-605856.03	±612.38	-478314.93	±531.02
85000	35446.23	±706.79	127629.78	±398.57	-606125.94	±405.27	-477988.34	±357.15
90000	35036.80	±230.09	127879.09	±425.58	-605938.91	±486.29	-477577.82	±452.78
95000	35100.63	±261.89	127409.73	±449.25	-606042.63	±515.98	-478126.02	±513.01
100000	34382.58	±572.34	127594.93	±376.68	-605226.04	±533.65	-477143.61	±476.53

Detailed analysis of these parameters is given in previous studies [37,38]. If these two parameters' numerical value becomes zero, it is expected that this inhibitor will be used as a drug in the future.

Molecular docking calculations for nanosecond-level binding calculations between molecule and protein have some drawbacks. In molecular docking calculations, although inhibitors are very flexible, proteins are not flexible at all. Molecular mechanics-Poisson-Boltzmann surface area (MM-PSBA) calculations are used to examine the interaction between molecule and protein in more detail. With these calculations, flexibility is given to both proteins and inhibitors. In these calculations, the protein and inhibitor are too surrounded by solvent molecules. In this study, the binding stability of protein-inhibitory structures was found for every five nanoseconds due to calculations. The Gibbs free energy value of the 4a inhibitor against 6X6P protein with the best docking score value was calculated. As a result of these calculations, the binding free energy changes and their deviations values were calculated for each five ns. There are many

interactions between protein and ligand. The most important interaction among these interactions is the hydrogen bond, which is one of the basic elements responsible for molecular interactions in biological systems [24]. The van der Waals energy (VDW), kinetic energy, potential energy, and Gibbs binding free energy changes of the inhibitor 4a against 6X6P protein were calculated. The final binding energy between protein and ligand is a cumulative sum of van der Waals, electrostatic, polar solvation, and SASA energy. An illustration of the interaction between protein and inhibitor is given at between 0-100 ns every 25 ns, in figure 9. These values are given in Table 3. Calculations made with molecular mechanics-Poisson-Boltzmann surface area (MM-PBSA) method were made to support molecular docking calculations. The more negative values obtained in these calculations indicate better binding [39-43]. The numerical values obtained from the calculations were plotted and given in Figure 10.

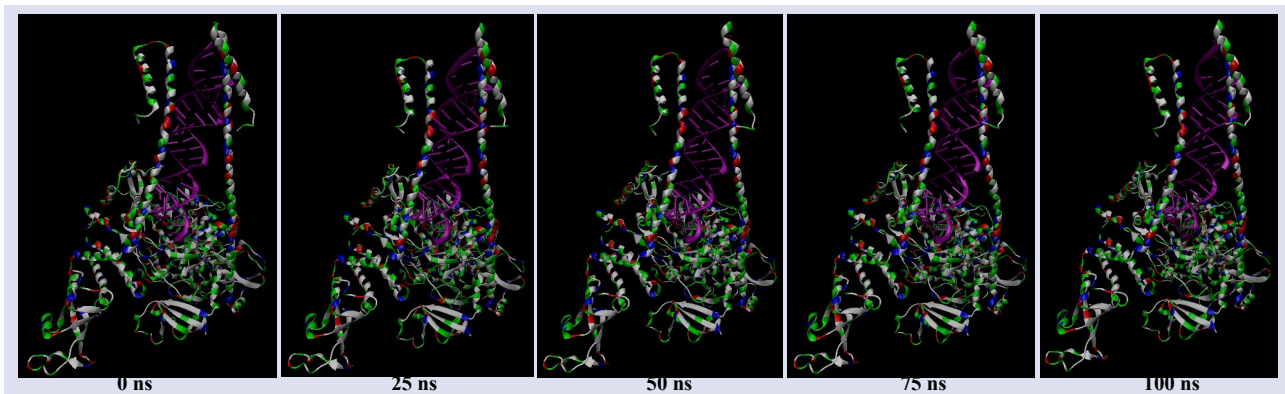


Figure 9. Representation of the interaction between protein and inhibitor is given at between 0-100 ns every 25 ns

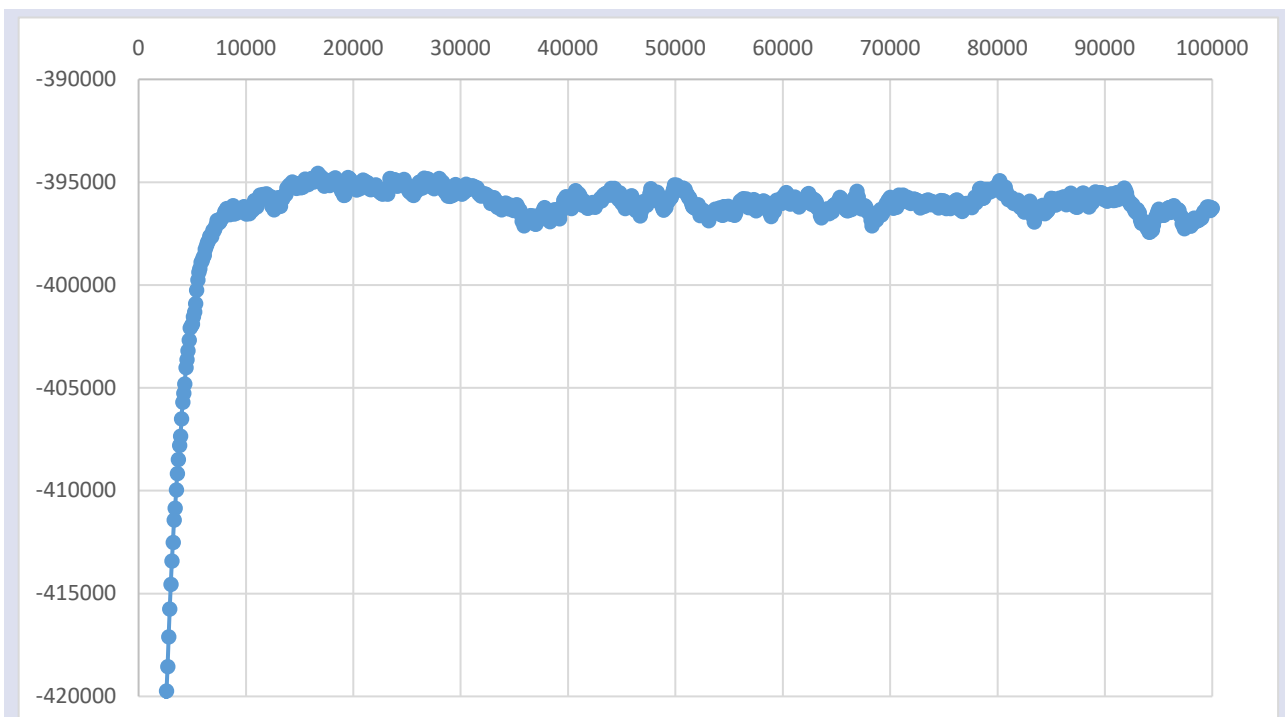


Figure 10. Change of Gibbs free energy values of 6X6P protein and molecule 5a in every five ns intervals.

As a result of the calculations, the inhibitory activities of 96 components of *Momordica Charantia* were compared against the SARS-CoV-2 virus. The calculated molecular dock results were compared with the values of corona drugs approved by the Food and Drug Administration (FDA) of the United States Ministry of

Health. Numerical values of FDA-approved drugs are given in Table 4. The structures of these FDA online drugs used were downloaded from the PubChem website (<https://pubchem.ncbi.nlm.nih.gov/>), and their calculations were made.

Table 4. Numerical values of the docking parameters of molecule against enzymes

Protein	Inhibitor	Docking score	Glide ligand efficiency	Glide evdw	Glide ecoul	Glide energy	Glide einternal	Glide emodel	Glide hBond
6X6P	37542	-5.59	-0.33	-21.05	-8.78	-29.83	3.00	-41.96	-2.62
6M0J	37542	-4.50	-0.26	-19.74	-5.20	-24.95	3.48	-37.19	-1.88
	84029	-2.57	-0.05	-20.46	-7.48	-27.94	15.61	10000	-1.18
	92727	-2.50	-0.05	-33.47	-11.57	-45.04	12.39	-58.92	-1.46
	131411	-1.38	-0.05	-27.55	-2.58	-30.12	3.80	-42.67	0.00
5RGG	37542	-4.26	-0.25	-12.66	-9.40	-22.06	4.27	-26.29	-2.68
	121304016	-3.19	-0.08	-37.43	-11.24	-48.66	9.35	-53.75	-1.63
	492405	-3.05	-0.28	-10.30	-7.91	-18.21	0.01	-21.00	-1.31
7BUY	92727	-6.13	-0.13	-45.13	-7.17	-52.30	13.77	-68.86	-1.18
	37542	-5.30	-0.31	-24.42	-8.92	-33.34	6.27	-40.09	-2.24
	492405	-4.53	-0.41	-17.50	-8.09	-25.59	0.01	-33.10	-1.79
7BV1	37542	-5.79	-0.34	-18.85	-15.86	-34.71	1.97	-43.45	-3.25
7BV2	37542	-6.94	-0.41	-15.81	-23.93	-39.74	3.44	-50.88	-4.38

These drugs are ribavirin (Pubchem number: 37542), arbidol (Pubchem number: 131411), favipiravir (Pubchem number: 492405), remdesivir (Pubchem number: 121304016), clarithromycin (Pubchem number: 84029), lopinavir (Pubchem number: 92727), and azithromycin (Pubchem number: 447043). These drugs are actively used against coronavirus. In the calculations for FDA approved drugs, the docking score of the ribavirin drug against the spike glycoprotein of the SARS-CoV-2 virus with 6X6P ID was -5.59, while the docking score value of the Karaviloside III (4a) inhibitor of *Momordica Charantia* was -9.36. Although the docking score of the ribavirin drug against the spike glycoprotein of the SARS-CoV-2 virus with 6M0J ID was -4.50, the docking score of *Momordica Charantia*'s Gypsogenin (2a) inhibitor was -3.34. In the next protein, the docking score value of the ribavirin drug against the main protease protein of the SARS-CoV-2 virus with 5RGG ID was -4.26, while the docking score value of the Karaviloside III (4a) inhibitor of *Momordica Charantia* was -6.20. Although the docking score of the lopinavir drug against the main protease protein of the SARS-CoV-2 virus with 7BUY ID was -6.13, the docking score value of the Karaviloside III (4a) inhibitor of *Momordica Charantia* was -7.35. In the next protein, the ribavirin drug's docking score against the RNA dependent RNA polymerase (RdRp) protein of the 7BV1 ID SARS-CoV-2 virus was -5.79 while the docking score value of *Momordica Charantia*'s Karaviloside III (4a) inhibitor was -8.42. Although the docking score value of ribavirin drug against RNA dependent RNA polymerase (RdRp) protein of SARS-CoV-

2 virus with 7BV2 ID was -4.68, *Momordica Charantia*'s momordicine I (3a) inhibitor had a docking score of -6.20.

As a result of the calculations, the covid-19 inhibitory activities of the molecules were compared. In many previous studies, the activity comparison of molecules was made. In the study of Aktaş et al. [44], RNA dependent RNA polymerase (RdRp) proteins were targeted, 3-Hydroxypyrazine-2-Carboxamide (CID 294642) and 2-oxo-(1,4-15N2)1H-pyrazine-3-(15N). The inhibitory activities of)carboxamide (CID 76973015) molecules were found to have higher inhibitory activity than the molecules studied. In the study of Ataseven et al. [45], the inhibitory activities of many boron molecules against spike glycoprotein, main protease and RNA dependent RNA polymerase of SARS-CoV-2 proteins were compared. ((R)-1-((S)-3-(4-(aminomethyl)phenyl)-2-benzamidopropanamido)-4-guanidinobutyl) boronic acid molecule was found to have higher inhibitory activity than other molecules. In the study by Tuzun et al. [46], the inhibitory activity of molecules in *Peganum harmala* extract was investigated to compare the inhibitory activities of SARS-CoV-2 against main protease, spike glycoproteins and RNA-dependent RNA polymerase proteins. It was observed that 1-methyl-1-Methyl-9H-beta-carbolin-7-ol molecule had higher inhibitory activity than other molecules against RNA-dependent RNA polymerase (RdRp) protein. In the study of Gedikli et al. [47], Inhibitory activities of SARS-CoV-2 virus against spike glycoprotein (PDB ID: 6M0J, 6LZG), main protease (PDB ID: 5RGG, 6WTT), and RNA dependent RNA polymerase (RdRp) (PDB ID: 6YYT, 7BV2) proteins were studied, Carvedilol molecule was found to have

higher inhibitory activity than other molecules. Çetiner et al. [48], in their study on boron-containing compounds, compared the inhibitory activities of SARS-CoV-2 against main protease, spike glycoproteins and RNA-dependent RNA polymerase proteins. The 4,6-di-tert-butyl-2-(4-methoxyphenyl) benzo[d][1,3,2] molecule was found to have higher inhibitory activity than other molecules. In the study of gedikli et al. [49], the inhibitory activities of clarithromycin, azithromycin and their analogues against the proteins of SARS-CoV2 virus were compared. In the comparison of SARS-CoV-2 virus against RNA-dependent RNA polymerase proteins, it is seen that Desosaminylazithromycin molecule has higher activity than other molecules. Many molecules have been studied in the above studies. Each molecule was found to have different activity in different SARS-CoV-2 protein regions.

Conclusion

A comparison of the inhibitory activities of *Momordica Charantia* against SARS-CoV-2 was performed for 96 components found in the extract. ADME / T analysis of molecules with high inhibitory activity was performed using the molecular docking method used for this comparison. Based on these results, MM-PBSA calculations were made for the molecule with the highest inhibitory activity. MM-PBSA calculations confirmed molecular docking results. Finally, by making a comparison with FDA approved medicines; Results show that the Karaviloside III (4a) inhibitor is a better inhibitor than other inhibitors and FDA approved drugs. It is recommended that the Karaviloside III (4a) inhibitor be used as an inhibitor in future in vivo and in vitro studies.

Acknowledgments

This work is supported by the Scientific Research Project Fund of Sivas Cumhuriyet University under the project number RGD-020. This research was made possible by TUBITAK ULAKBIM, High Performance, and Grid Computing Center (TR-Grid e-Infrastructure).

Conflict of Interest

No potential conflict of interest was reported by the author(s).

References

- [1] Gorbalenya A.E., Baker S.C., Baric R., Groot R.J.D., Drosten C., Gulyaeva A.A., ... Ziebuhr J., Severe acute respiratory syndrome-related coronavirus: Classifying 2019-NCoV and naming it SARS-CoV-2, *Nature Microbiology*, (2020) 1–9.
- [2] Alagaili A.N., Briese T., Mishra N., Kapoor V., Sameroff S.C., de Wit E., ... Lipkin W.I., Middle East respiratory syndrome coronavirus infection in dromedary camels in Saudi Arabia, *MBio*, 5(2) (2014) e00884-14.
- [3] Chen N., Zhou M., Dong X., Qu J., Gong F., Han Y., ... Zhang L., Epidemiological and clinical characteristics of 99 cases of 2019 novel coronavirus pneumonia in Wuhan, China: a descriptive study, *The Lancet*, 395(10223) (2020) 507-513.
- [4] Ahmed F.S., Quadeer A.A., McKay R.M., Preliminary identification of potential vaccine targets for the COVID-19 coronavirus (SARS-CoV-2) based on SARS-CoV immunological studies, *Viruses*, 12(3) (2020) 254.
- [5] Tao Y., Shi M., Chommanard C., Queen K., Zhang J., Markotter W., ... Tong S., Surveillance of bat coronaviruses in Kenya identifies relatives of human coronaviruses NL63 and 229E and their recombination history, *Journal of Virology*, 91(5) (2017) e01953–16.
- [6] Wang D., Hu B., Hu C., Zhu F., Liu X., Zhang J., ... Peng Z., Clinical characteristics of 138 hospitalized patients with 2019 novel coronavirus-infected pneumonia in Wuhan, China, *JAMA*, 323(11) (2020) e201585.
- [7] Wang M., Cao R., Zhang L., Remdesivir and chloroquine effectively inhibit the recently emerged novel coronavirus (2019-nCoV) in vitro, *Cell Res.*, 30(3) (2020) 269-271.
- [8] Gallagher T.M., Buchmeier M.J., Coronavirus spike proteins in viral entry and pathogenesis, *Virology*, 279(2) (2001) 371–374.
- [9] Ahn D.G., Shin H.J., Kim M.H., Lee S., Kim H.S., Myoung J., ... Kim S.J., Current status of epidemiology, diagnosis, therapeutics, and vaccines for novel coronavirus disease 2019 (COVID-19), *Journal of Microbiology and Biotechnology*, 30(3) (2020) 313–324.
- [10] Schoeman D., Fielding B.C., Coronavirus envelope protein: Current knowledge, *Virology Journal*, 16(1) (2019) 69.
- [11] Sheahan T.P., Sims A.C., Leist S.R., Schäfer A., Won J., Brown A.J., ... Baric R.S. Comparative therapeutic efficacy of remdesivir and combination lopinavir, ritonavir, and interferon beta against MERS-CoV Nat., *Commun.*, 11(1) (2020) 1-14.
- [12] Maxmen A., More than 80 clinical trials launch to test coronavirus treatments, *Nature*, 578(7795) (2020) 347–348.
- [13] Arabi Y.M., Shalhoub S., Mandourah Y., Al-Hameed F., Al-Omari A., Al Qasim E., ... Fowler R., Ribavirin and Interferon Therapy for Critically Ill Patients with Middle East Respiratory Syndrome: A Multicenter Observational Study, *Clin. Infect. Dis.*, 70(9) (2019) 1837-1844.
- [14] Lakhri Y., Rbaa M., Tuzun B., Hichar A., Ounine K., Almalki F., Lakhri B., Synthesis, structural confirmation, antibacterial properties and bio-informatics computational analyses of new pyrrole based on 8-hydroxyquinoline, *Journal of Molecular Structure*, 1259 (2022) 132683.
- [15] Al-Janabi I.A.S., Yavuz S.Ç., Köprü S., Tapera M., Kekeçmuhammed H., Akkoç S., ... Sarıpinar, E. Antiproliferative activity and molecular docking studies of new 4-oxothiazolidin-5-ylidene acetate derivatives containing guanylhydrazone moiety, *Journal of Molecular Structure*, 1258 (2022) 132627.
- [16] Ahamad J., Amin S., Mir S.R., *Momordica charantia* Linn.(Cucurbitaceae): Review on phytochemistry and pharmacology, *Phytochemistry*, 11(2) (2017) 53-65.
- [17] Jiratchariyakul W., Wiwat C., Vongsakul M., Somanabandhu A., Leelamanit W., Fujii I., ... Ebizuka Y., HIV inhibitor from Thai bitter gourd, *Planta Medica*, 67(04) (2001) 350-353.
- [18] Nerurkar P., Ray R.B. Bitter melon: antagonist to cancer, *Pharmaceutical Research*, 27(6) (2010) 1049-1053.
- [19] Pitchakarn P., Ogawa K., Suzuki S., Takahashi S., Asamoto M., Chewonarin T., Shirai T., *Momordica charantia* leaf extract suppresses rat prostate cancer progression in vitro and in vivo, *Cancer Science*, 101(10) (2010) 2234-2240.

- [20] Frisch M.J., Trucks G.W., Schlegel H.B., Scuseria G.E., Robb M.A., Cheeseman J.R., Scalmani G., Barone V., Mennucci B., Petersson G.A., Nakatsuji H., Caricato M., Li X., Hratchian H.P., Izmaylov A.F., Bloino J., Zheng G., Sonnenberg J.L., Hada M., Ehara M., Toyota K., Fukuda R., Hasegawa J., Ishida M., Nakajima T., Honda Y., Kitao O., Nakai H., Vreven T., Montgomery J.A., Peralta J.E., Ogliaro F., Bearpark M., Heyd J.J., Brothers E., Kudin K.N., Staroverov V.N., Kobayashi R., Normand J., Raghavachari K., Rendell A., Burant J.C., Iyengar S.S., Tomasi J., Cossi M., Rega N., Millam J.M., Klene M., Knox J.E., Cross J.B., Bakken V., Adamo C., Jaramillo J., Gomperts R., Stratmann R.E., Yazyev O., Austin A.J., Cammi R., Pomelli C., Ochterski J.W., Martin R.L., Morokuma K., Zakrzewski V.G., Voth G.A., Salvador P., Dannenberg J.J., Dapprich S., Daniels A.D., Farkas O., Foresman J.B., Ortiz J.V., Cioslowski J., Fox D.J. (2009) Gaussian 09, revision D.01. Gaussian Inc, Wallingford CT.
- [21] Schrödinger L. (2019). Small-Molecule Drug Discovery Suite 2019-4.
- [22] Schrödinger Release (2019) 2019-4: Protein Preparation Wizard; Epik, Schrödinger, LLC, New York, NY, 2016; Impact, Schrödinger, LLC, New York, NY, 2016; Prime, Schrödinger, LLC, New York, NY.
- [23] Rbaa M., Haida S., Tuzun B., El Hassane A., Kribii A., Lakhrissi Y., ... Berdimurodov E., Synthesis, characterization and bioactivity of novel 8-hydroxyquinoline derivatives: Experimental, molecular docking, DFT and POM analyses, *Journal of Molecular Structure*, 1258 (2022) 132688.
- [24] Schrödinger Release (2019) 2019-4: LigPrep, Schrödinger, LLC, New York, NY, 2019.
- [25] Kökbudak Z., Akkoç S., Karataş H., Tüzün B., Aslan G. In Silico and In Vitro Antiproliferative Activity Assessment of New Schiff Bases, *Chemistry Select*, 7(3) (2022) e202103679.
- [26] Koçyiğit Ü.M., Taslimi P., Tüzün B., Yakan H., Muğlu H., Güzel E., 1, 2, 3-Triazole substituted phthalocyanine metal complexes as potential inhibitors for anticholinesterase and antidiabetic enzymes with molecular docking studies, *Journal of Biomolecular Structure and Dynamics*, (2020) 1-11.
- [27] Schrödinger Release 2020-1: QikProp, Schrödinger, LLC, New York, NY, 2020.
- [28] Nelson M.T., Humphrey W., Gursoy A., Dalke A., Kalé L.V., Skeel R.D., Schulten K., NAMD: A parallel, object-oriented molecular dynamics program, *The International Journal of Supercomputer Applications and High-Performance Computing*, 10(4) (1996) 251–268.
- [29] Humphrey W., Dalke A., Schulten K., VMD: Visual molecular dynamics, *Journal of Molecular Graphics*, 14(1) (1996) 33–38.
- [30] Celebioglu H.U., Erden Y., Hamurcu F., Taslimi P., Şentürk O.S., Özmen, Ü.Ö., ... Gulçin İ., Cytotoxic effects, carbonic anhydrase isoenzymes, α -glycosidase and acetylcholinesterase inhibitory properties, and molecular docking studies of heteroatom-containing sulfonyl hydrazone derivatives, *Journal of Biomolecular Structure and Dynamics*, (2020) 1-12.
- [31] Huseynova A., Kaya R., Taslimi P., Farzaliyev V., Mammadyarova X., Sujayev, A., ... Gulçin İ. Design, synthesis, characterization, biological evaluation, and molecular docking studies of novel 1, 2-aminopropanthiols substituted derivatives as selective carbonic anhydrase, acetylcholinesterase and α -glycosidase enzymes inhibitors, *Journal of Biomolecular Structure and Dynamics*, (2020) 1-13.
- [32] Taslimi P., Erden Y., Mamedov S., Zeynalova L., Ladokhina N., Tas R., ... Gulçin İ., The Biological Activities, Molecular Docking Studies, and Anticancer Effects of 1-Arylsulphonylpyrazole Derivatives, *Journal of Biomolecular Structure and Dynamics*, (2020) 1-20.
- [33] Demir Y., Taslimi P., Koçyiğit Ü. M., Akkuş M., Özaslan M. S., Duran H. E., et al., Determination of the inhibition profiles of pyrazolyl-thiazole derivatives against aldose reductase and α -glycosidase and molecular docking studies, *Archiv der Pharmazie*, (2020) e2000118.
- [34] Lipinski C. A., Lead-and drug-like compounds: the rule-of-five revolution, *Drug Discovery Today: Technologies*, 1(4) (2004) 337-341.
- [35] Lipinski C. A., Lombardo F., Dominy B. W., Feeney P. J., Experimental and computational approaches to estimate solubility and permeability in drug discovery and development settings, *Advanced Drug Delivery Reviews*, 23 (1997) 3-25.
- [36] Jorgensen W.J., Duffy E.M., Prediction of drug solubility from structure, *Advanced Drug Delivery Reviews*, 54(3) (2002) 355-366.
- [37] Kısa D., Korkmaz N., Taslimi P., Tuzun B., Tekin Ş., Karadağ A., Şen F., Bioactivity and Molecular Docking Studies of Some Nickel Complexes: New Analogues for the Treatment of Alzheimer, Glaucoma and Epileptic Diseases, *Bioorganic Chemistry*, (2020) 104066.
- [38] Türkan F., Taslimi P., Abdalrazaq S. M., Aras A., Erden Y., Celebioglu H. U., et al., Determination of anticancer properties and inhibitory effects of some metabolic enzymes including acetylcholinesterase, butyrylcholinesterase, alpha glycosidase of some compounds with molecular docking study, *Journal of Biomolecular Structure and Dynamics*, (2020) 1-17.
- [39] Alici E.H., Bilgiçli A.T., Tüzün B., Günşel A., Arabaci G., Yarasir M.N., Alkyl chain modified metalophthalocyanines with enhanced antioxidant-antimicrobial properties by doping Ag⁺ and Pd²⁺ ions, *Journal of Molecular Structure*, 1257 (2022) 132634.
- [40] Erdogan M.K., Gundogdu R., Yapar Y., Gecibesler I.H., Kirici M., Behcet L., ... Taslimi P., The Evaluation of Anticancer, Antioxidant, Antidiabetic and Anticholinergic Potentials of Endemic Rhabdosciadium microcalycinum Supported by Molecular Docking Study, *ChemistrySelect*, 7(17) (2022) e202200400.
- [41] Majumdar D., Tüzün B., Pal T.K., Das S., Bankura K., Architectural View of Flexible Aliphatic-OH Group Coordinated Hemi-Directed Pb (II)-Salen Coordination Polymer: Synthesis, Crystal Structure, Spectroscopic Insights, Supramolecular Topographies, and DFT Perspective, *Journal of Inorganic and Organometallic Polymers and Materials*, (2022) 1-18.
- [42] Shafiee S., Davaran S., A mini-review on the current COVID-19 therapeutic strategies, *Chemical Review and Letters*, 3(1) (2020) 19-22.
- [43] Majedi S., Majedi S., Existing drugs as treatment options for COVID-19: A brief survey of some recent results, *Journal of Chemistry Letters*, 1(1) (2020) 2-8.
- [44] Aktaş A., Tüzün B., Aslan R., Sayin K., Ataseven H., New anti-viral drugs for the treatment of COVID-19 instead of favipiravir, *Journal of Biomolecular Structure and Dynamics*, 39(18) (2021) 7263-7273.

- [45] Ataseven H., Sayin K., Tüzün B., Gedikli M., Could boron compounds be effective against SARS-CoV-2?, *Bratislava Medical Journal-Bratislavské Lekárske Listy*, 122(10) (2021) 753-758.
- [46] Tuzun B., Nasibova T., Garaev E., Sayin K., Ataseven H. Could Peganum harmala be effective in the treatment of COVID-19?, *Bratislavské Lekárske Listy*, 122(9) (2021) 670-679.
- [47] Gedikli M.A., Tuzun B., Sayin K., Ataseven H., Determination of inhibitor activity of drugs against the COVID-19, *Bratislavské Lekárske Listy*, 122(7) (2021) 497-506.
- [48] Cetiner E., Sayin K., Tuzun B., Ataseven H., Could boron-containing compounds (BCCs) be effective against SARS-CoV-2 as anti-viral agent?, *Bratislavské Lekárske Listy*, 122(4) (2021) 263-269.
- [49] Gedikli M., Tuzun, B., Aktas A., Sayin K., Ataseven H., Are clarithromycin, azithromycin and their analogues effective in the treatment of COVID19, *Bratislava Medical Journal-Bratislavské Lekárske Listy*, 122(2) (2021) 101-110.